

# Self-consistent Determination of Temperature and Fluctuation Thermometer in Heavy-ion Reactions near the Fermi Energies

X. Liu,<sup>1,2,\*</sup> W. Lin,<sup>1,2</sup> R. Wada,<sup>1,†</sup> M. Huang,<sup>1</sup> Z. Chen,<sup>1</sup> G. Q. Xiao,<sup>1</sup> S. Zhang,<sup>1,2</sup> X. Jin,<sup>1,2</sup> R. Han,<sup>1</sup> J. Liu,<sup>1</sup> F. Shi,<sup>1</sup> P. Ren,<sup>2,1</sup> H. Zheng,<sup>3,4</sup> J. B. Natowitz,<sup>3</sup> and A. Bonasera<sup>3,5</sup>

<sup>1</sup>*Institute of Modern Physics, Chinese Academy of Sciences, Lanzhou, 730000, China*

<sup>2</sup>*University of Chinese Academy of Sciences, Beijing 100049, China*

<sup>3</sup>*Cyclotron Institute, Texas A&M University, College Station, Texas 77843*

<sup>4</sup>*Physics Department, Texas A&M University, College Station, Texas 77843*

<sup>5</sup>*Laboratori Nazionali del Sud, INFN, via Santa Sofia, 62, 95123 Catania, Italy*

(Dated: June 8, 2019)

The density and temperature of a fragmenting system in a multifragmentation process are evaluated in a self-consistent manner using ratios between the ratio of the symmetry energy coefficient relative to the temperature,  $a_{sym}/T$ , extracted from the fragment yields generated by antisymmetrized molecular dynamics (AMD) simulations for central collisions of  $^{40}\text{Ca} + ^{40}\text{Ca}$  at 35 MeV/nucleon. The  $a_{sym}/T$  values are extracted from all isotope yields by an improved method based on the Modified Fisher Model (MFM). The ratios of  $a_{sym}/T$  obtained, using interactions with different density dependencies of the symmetry energy term, reflect the ratios of the symmetry energy at the density of fragment formation. Using this correlation, the density is found to be  $\rho/\rho_0 = 0.66 \pm 0.02$ . The symmetry energy values for each interaction are determined at this density. With these values, temperature values are extracted as a function of isotope mass  $A$ . The extracted temperature values are compared with those evaluated from the fluctuation thermometer with a radial flow correction.

PACS numbers: 25.70.Pq

Keywords: Intermediate heavy ion reactions, multifragmentation, density, temperature, fluctuation thermometer, antisymmetrized molecular dynamics model

## I. Introduction

A wealth of nuclear phenomena, including dynamical processes in nuclear reactions, nuclear structure and nuclear astrophysics are intimately affected by the density dependence of the symmetry energy term in the nuclear equation of state (EOS) [1]. Investigations of the symmetry energy, especially focusing on its density dependence, have been conducted using many observables such as isotopic yield ratios [2], isospin diffusion [3], neutron-proton emission ratios [4], giant monopole resonances [5], pygmy dipole resonances [6], giant dipole [7], collective flow [8] and isoscaling [9–11]. The ratio of the symmetry energy coefficient relative to the temperature,  $a_{sym}/T$ , extracted from the isotope yield ratios [12, 13], has been extracted within the frame work of the Modified Fisher Model (MFM) [14–17].

While temperature is one of the key variables in characterizing the mechanisms of the nuclear reactions, it is very difficult to determine the temperature of a hot nuclear matter in a dynamical process. Several nuclear thermometers have been proposed. These include the slope of energy spectra [18, 19], momentum fluctuations [20], double isotope yield ratios [21] and excited state distributions [22] among others. However even for a given system the extracted temperature values from these thermometers may be quite different from each other [23] and they may not be generally applicable in all circumstances.

In our recent work, the isotopic yield method was applied to extract the value of  $a_{sym}/T$  values from the ex-

perimentally reconstructed primary fragment yields and compared to those calculated for AMD primary generated fragment yields obtained using Gogny interactions with different density dependencies of the symmetry energy [24]. In the analysis, we found that the extracted  $a_{sym}/T$  values change according to the interactions used. From the dependence on interaction, the density, symmetry energy and temperature at the time of fragment formation were determined in a self-consistent manner. In this paper we use the same procedure to determine these parameters for the central collision events ( $b = 0\text{fm}$ ) of  $^{40}\text{Ca} + ^{40}\text{Ca}$  at 35 A MeV, generated by AMD with interactions having different density dependencies of the symmetry energy term, i.e., the standard Gogny interaction (g0), the Gogny interaction with an asymptotic stiff symmetry energy (g0AS) and the Gogny interaction with an asymptotic super-stiff symmetry energy (g0ASS) [25, 26]. The extracted temperature values are compared to those obtained using a fluctuation thermometer.

## II. MFM Model and Extraction of $a_{sym}/T$

In Ref. [12] only yields of isotopes with  $I = N - Z = -1, 1$  and 3 were used to extract the ratio of the symmetry energy coefficient relative to the temperature,  $a_{sym}/T$ . In this article, an improved method for the extraction is used. In the improved method, all available isotope yields are employed. The improvement is made possible by taking into account the volume, sur-

face, Coulomb, pairing and chemical potential terms explicitly in the free energy. In the framework of MFM, the yield of an isotope with  $N$  neutrons and  $Z$  protons produced in a multi-fragmentation reaction, can be given as [11, 12, 15–17, 27]

$$Y(N, Z) = Y_0 \cdot A^{-\tau} \exp\left[\frac{W(N, Z) + \mu_n N + \mu_p Z}{T}\right] + N \ln\left(\frac{N}{A}\right) + Z \ln\left(\frac{Z}{A}\right). \quad (1)$$

Using the generalized Weiszäcker-Beth semiclassical mass formula [28, 29],  $W(N, Z)$  can be approximated as

$$W(N, Z) = a_v A - a_s A^{2/3} - a_c \frac{Z(Z-1)}{A^{1/3}} - a_{sym} \frac{(N-Z)^2}{A} - a_p \frac{\delta}{A^{1/2}}, \quad (2)$$

$$\delta = -\frac{(-1)^Z + (-1)^N}{2}.$$

In Eq.(1),  $A^{-\tau}$  and  $N \ln(N/A) + Z \ln(Z/A)$  originate from the increases of the entropy and the mixing entropy at the time of the fragment formation, respectively.  $\mu_n$  ( $\mu_p$ ) is the neutron (proton) chemical potential.  $\tau$  is the critical exponent. In this work, the value of  $\tau = 2.3$  is adopted from the previous studies [17]. In general coefficients,  $a_v$ ,  $a_s$ ,  $a_{sym}$ ,  $a_p$  and the chemical potentials are temperature and density dependent, even though these dependence are not shown explicitly.

Initially we apply Eq.(1) to the isotopes with  $N = Z$ . For  $N = Z = A/2$  isotopes, the free energy relative to the temperature can be calculated from Eq.(1) and Eq.(2) as

$$-\frac{F(A/2, A/2)}{T} = \ln\left[\frac{Y(A/2, A/2)A^\tau}{Y_0}\right] = \frac{\widetilde{a}_v}{T} A - \frac{a_s}{T} A^{2/3} - \frac{a_c}{T} \frac{A(A-2)}{4A^{1/3}} - \frac{a_p}{T} \frac{\delta}{A^{1/2}} + A \ln\left(\frac{1}{2}\right), \quad (3)$$

where  $\widetilde{a}_v = a_v + \frac{1}{2}(\mu_n + \mu_p)$ . The value of  $\ln\left[\frac{Y(A/2, A/2)A^\tau}{Y_0}\right]$  on the right of the first equation can be calculated from the experimental values when the  $\tau$  value is fixed. In order to eliminate  $Y_0$ , all isotope yields are normalized by the yield of  $^{12}\text{C}$  [11, 12, 17]. The renormalized values of  $-\frac{F(A/2, A/2)}{T}$  from the AMD events are plotted as a function of the isotope mass  $A$  using solid points in Fig. 1(a). The values of  $\widetilde{a}_v/T$ ,  $a_s/T$ ,  $a_c/T$  and  $a_p/T$  are used as free parameters to fit the given  $-\frac{F(A/2, A/2)}{T}$  values, employing Eq.(3). A typical search result is shown by open circles in Fig. 1(a) for the case of the g0 interaction. Similar quality results are obtained for the events generated using the g0AS and g0ASS interactions.

Secondly Eq.(1) is applied to yields of isotopes with  $N \neq Z$ . From Eq.(1),  $a_{sym}/T$  and  $\Delta\mu/T = (\mu_n - \mu_p)/T$

values can be related to the modified free energy,  $\frac{\Delta F(N, Z)}{T}$  as

$$\frac{\Delta F(N, Z)}{T} = \frac{a_{sym}}{T} \frac{(N-Z)^2}{A} - \frac{\Delta\mu}{2T} (N-Z), \quad (4)$$

where  $\frac{\Delta F(N, Z)}{T}$  is the free energy relative to the temperature,  $\frac{F(N, Z)}{T}$ , subtracted by the calculated contributions of the volume, surface, Coulomb and pairing terms, using the parameters extracted for  $N = Z$  isotopes above. Resultant  $\frac{\Delta F(N, Z)}{T}$  values are shown by symbols in Fig. 1(b). They exhibit quadratic shapes with the minimum values close to zero. The minimum values are closely related to  $\Delta\mu/T$  in Eq.(4) and therefore  $\Delta\mu/T \sim 0$  in the  $^{40}\text{Ca} + ^{40}\text{Ca}$  system. By fitting the quadratic shape assuming  $a_{sym}/T$  and  $\Delta\mu/T$  as free parameters,  $a_{sym}/T$  values are extracted and plotted in Fig. 1(c) separately for the g0, g0AS and g0ASS interactions. As one can see, in all cases the extracted  $a_{sym}/T$  values increase as  $Z$  increases, and they are more or less parallel each other. The  $a_{sym}/T$  values for  $Z = 2$  and 3 isotopes behave slightly differently from those of the heavier fragments. The AMD simulations indicate a significant pre-equilibrium contribution to the production of these light isotopes. Similar results are seen in other codes [30, 31]. Therefore, in the following analysis the isotopes with  $Z = 2$  and 3 are excluded and we focus on the yields of the heavier isotopes.

### III. Self-consistent Determination of Density and Temperature

In order to determine the density and temperature at the time of the fragment formation, the parallel behavior of the observed  $a_{sym}/T$  values in Fig. 1(c) is utilized. As suggested in Ref. [26], the observed parallel behavior is attributed to the difference of the symmetry energy at the density at the time of the fragment formation. The ratios of  $a_{sym}/T$  values between g0/g0AS and g0/g0ASS are shown in Fig. 2(a). The ratios show flat distributions as a function of  $Z$  for both cases. The extracted average ratio values are shown in the first column of Table I. In Fig. 2(b) the symmetry energy coefficient is plotted as a function of the density for the three interactions used in the calculations and in Fig. 2(c) their ratios,  $R_{sym} = a_{sym}(g0)/a_{sym}(g0AS)$  and  $R_{sym} = a_{sym}(g0)/a_{sym}(g0ASS)$ , are plotted. Using the ratio values determined from Fig. 2(a) and the density dependence of the  $R_{sym}$  values in Fig. 2(c), the implied densities of the fragmenting system is indicated by the shaded vertical areas shown in Fig. 2(c). The extracted density values for each case are given in the second column of Table I. Assuming that the nucleon density should be for the three different interactions used, the nucleon density of the fragmenting system is determined as the

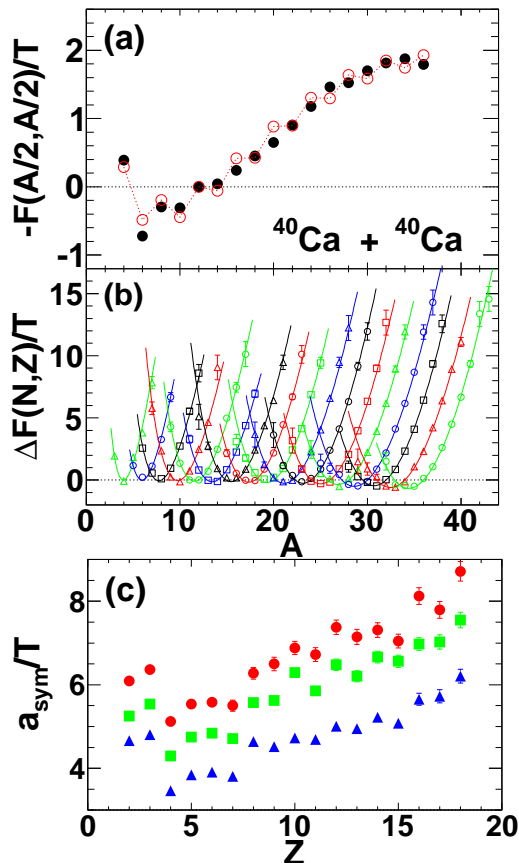


FIG. 1: (color online) (a) Calculated ratio of free energy to  $T$  for  $N = Z$  isotopes from the AMD events with  $g_0$  (solid points). Circles represent the fit using Eq.(3). The parameters extracted are  $\bar{a}_v/T = 2.65$ ,  $a_s/T = 4.86$ ,  $a_c/T = 0.22$ ,  $a_p/T = 0.48$ . (b) Calculated  $\frac{\Delta F(N,Z)}{T}$  values and quadratic fits using Eq.(4) for  $Z = 2$  to 18. The same symbols are used for isotopes with a given  $Z$ . (c) Extracted  $a_{sym}/T$  values from (b) for  $g_0$  (dots),  $g_0AS$  (squares) and  $g_0ASS$  (triangles).

overlap of the extracted values. This assumption is reasonable because the nucleon density is mainly determined by the stiffness of the EOS and not by the density dependence of the symmetry energy term. From the overlapped density area in Fig. 2(c),  $\rho/\rho_0 = 0.66 \pm 0.02$  is evaluated as the density at the time of the fragment formation. Using this density value, the corresponding symmetry energy values at that density are extracted for the three different interactions from Fig. 2(b). They are given in the third column of Table I.

Once the symmetry energy value is determined for a given interaction, the temperature,  $T_{sym}$ , can be calculated as  $T_{sym} = a_{sym} / (a_{sym}/T)$ . The results are shown by closed symbols in Fig. 3(b) by dots( $g_0$ ), squares ( $g_0AS$ ) and triangles ( $g_0ASS$ ). The results are plotted as a function of mass  $A$ , using the approximation  $A \approx 2Z$ , for the comparisons to those of the model simulation described below. The temperature values extracted from the three different interactions agree with each other very

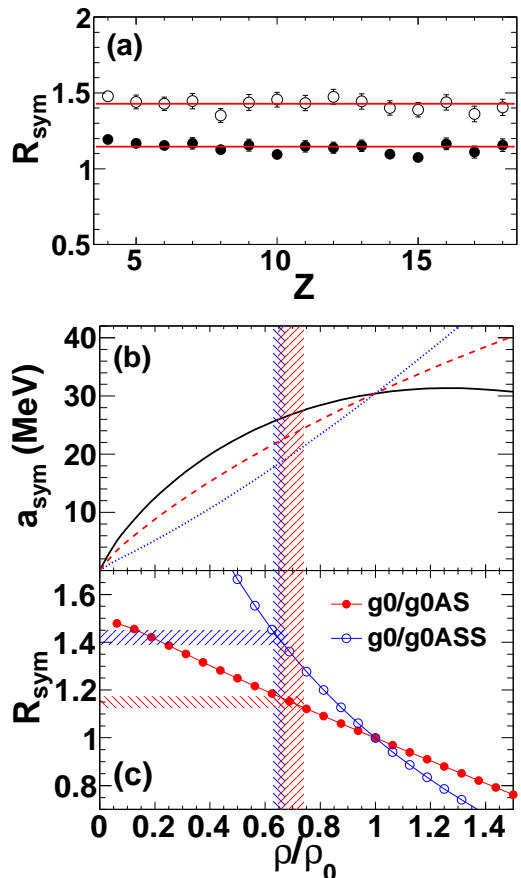


FIG. 2: (color online) (a) The ratios of the  $a_{sym}/T$  values shown in Fig. 1(c), dots for  $g_0/g_0AS$  and circles for  $g_0/g_0ASS$ . (b) Symmetry energy coefficient vs density used in the AMD simulations. Solid curve( $g_0$ ), dashed ( $g_0AS$ ) and dotted ( $g_0ASS$ ) (c) The ratio of the symmetry energy coefficient in (b). The shaded horizontal lines are the ratios extracted in (a) and the vertical shaded area is the density region corresponding the ratios. Two different shadings are used for the two ratio values.

TABLE I: Extracted parameters

	Ratio	$\rho/\rho_0$	$a_{sym}$ (MeV)
$g_0$			$26.2 \pm 0.4$
$g_0/g_0AS$	$1.15 \pm 0.02$	$0.69 \pm 0.05$	
$g_0AS$			$23.2 \pm 1.3$
$g_0/g_0ASS$	$1.42 \pm 0.03$	$0.65 \pm 0.02$	
$g_0ASS$			$18.4 \pm 0.7$

well and show a monotonic decrease as  $A$  increases from  $T \sim 5$  MeV at  $A = 8$  to  $T \sim 3$  MeV at  $A = 36$ . The decreasing trend as  $A$  increases is often observed in heavy ion collisions and normally attributed to variations in impact parameter [32]. The heavier fragments tend to be produced in more peripheral collisions and therefore show lower temperature. However in this study all events analyzed are generated in the same class of events, central collisions with  $b = 0$  fm. Therefore the decreasing trend

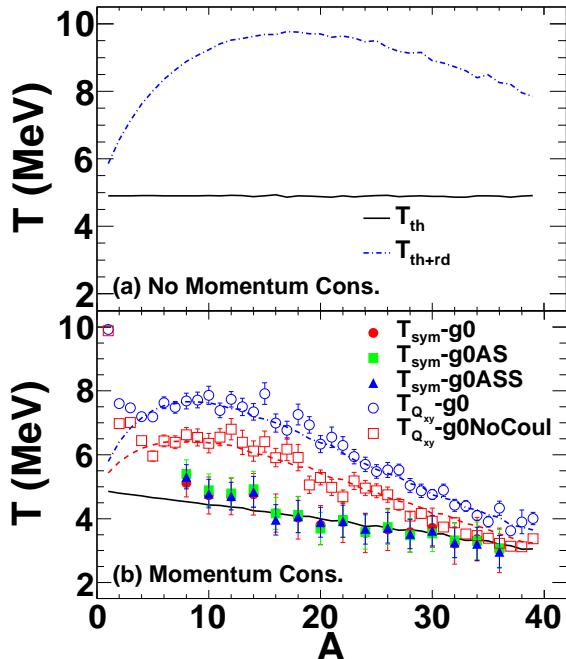


FIG. 3: (color online) (a) Temperatures from the Monte-Carlo model calculation. The solid curve represents the fluctuation temperature values for a thermally equilibrated system using  $T_0 = 4.9$  MeV. The dashed curve represents those corresponding to the system with additional radial flow with  $k = 0.024$  c/fm. No momentum conservation is applied. (b) Temperature values extracted in different methods. Closed symbols (dots, squares, triangles) represent the temperature values from the self-consistent symmetry energy analysis, using the AMD events. Open circles represent the fluctuation temperature values,  $T_{Q_{xy}}$ . Open squares represent those from the AMD events with no Coulomb potential. Solid and dashed curves are those similar to (a) but under the condition of the momentum conservation.

may originate in different fragment formation processes rather than in the centrality of the events.

#### IV. Discussion

The temperature at the time of the fragment formation has been studied, using different thermometers [23], such as the population of the excited states [22], double isotope yield ratios [21], the slopes of energy spectra [18, 19], the fluctuations of momentum distributions [20] among others. Here we will investigate the applicability of the fluctuation thermometer using different isotopes.

For a given variable  $X$ , the fluctuation is given as  $\sigma^2(X) = \langle X^2 \rangle - \langle X \rangle^2$ . In our present work, focusing on momentum fluctuations,  $X = Q_{xy} = P_x^2 - P_y^2$  is used, following Ref. [20]. Different relationships have been proposed to derive the temperature from observed momentum fluctuations. In Ref. [20] a classical relationship is assumed. In Refs. [33, 34], Zheng et al. reported that there may be significant effects on the fluctuation tem-

perature resulting from the quantum nature of the particles examined. When the temperature is determined from the fermions, such as n, p, t etc., the momentum distribution is expected to follow the Fermi-Dirac distribution [33]. On the other hand, when bosons, such as d or  $\alpha$  particles, are used, the Bose-Einstein distribution is expected to be appropriate [34]. In this paper the fluctuation temperature is calculated from IMF momentum distributions including those in the excited states from the primary fragments of AMD simulations without an afterburner. Fermions and bosons are mixed and therefore we assume the classical momentum distribution for the following analysis.

Under the assumption of the Maxwell-Boltzmann distribution, the momentum distribution is,

$$f(\vec{P}) = \frac{1}{(2m\pi T)^{3/2}} \exp\left(-\frac{\vec{P}^2}{2mT}\right), \quad (5)$$

and the fluctuation of  $Q_{xy}$ ,  $\sigma^2(Q_{xy})$ , can be given as

$$\sigma^2(Q_{xy}) = \frac{1}{(2m\pi T)^{3/2}} \int (P_x^2 - P_y^2)^2 f(\vec{P}) d\vec{P}. \quad (6)$$

From this one can show that  $\sigma^2(Q_{xy}) = 4m^2T^2$  for a given particle with mass  $m$ , and therefore the fluctuation temperature  $T_{Q_{xy}} = \sqrt{\sigma^2(Q_{xy})}/2m$  is obtained. The fluctuation temperature values calculated from the AMD events with the g0 interaction are represented by open circles in Fig. 3(b). Very similar results of the fluctuation temperature values are obtained for the other two interactions. As seen in the figure, over the entire range of isotope mass, the fluctuation temperature values are quite different from the  $T_{sym}$  values.  $T_{Q_{xy}} \sim 10$  MeV for  $A = 1$ , a shallow minimum with  $T_{Q_{xy}} \sim 7$  MeV around  $A \sim 4$  and a broad peak  $T_{Q_{xy}} \sim 8$  MeV around  $A \sim 12$ , and then a monotonic decrease as  $A$  increases. For comparison the fluctuation temperature values from the AMD events without the Coulomb interaction are also calculated and shown by open squares. They show a similar trend to those with the Coulomb interaction included, but about 1.0 to 1.5 MeV lower temperature in the entire mass range except for  $A = 1$ . Both temperature values for  $A = 1$  show  $T \sim 10$  MeV.

In order to understand the behavior of the extracted fluctuation temperature, simple Monte-Carlo calculations were performed. In this model, a percolation model was utilized to generate fragments from 80 lattice points ( $4 \times 4 \times 5$ ) [35]. No charge and internal excitation energy are considered in the percolation model. The motion of particles was assigned as the sum of the thermal motion and radial expansion. In the central AMD collisions ( $b = 0$  fm), collective contributions to the particle energy occur only in the radial direction. Both radial flow and Coulomb repulsion contribute to the radial expansion motion. The Coulomb acceleration is treated as a part of the radial flow and the radial velocity is defined

as  $\vec{v}^{rd} = k \vec{r}$ , where  $k$  is the flow parameter and  $\vec{r}$  is the coordinate vector. Fragments generated by the percolation model are distributed uniformly inside a sphere of radius  $r_{sys}$  under the condition of  $r \leq r_{sys} - r_A$ , where  $r_A$  is the radius of the fragment with mass  $A$ . They are calculated as  $r_{sym} = 1.2 \times [80/(\rho/\rho_0)]^{1/3}$  and  $r_A = 1.2 \times [A/(\rho/\rho_0)]^{1/3}$ , where  $\rho/\rho_0 = 0.66$  is adopted from the above analysis. This condition allows some overlap of two spheres but for the purpose of the restriction of the  $r$  distribution, this condition is good enough to see the global effect of the fluctuation temperature. Under a thermal equilibrium condition, the thermal velocity  $v_i^{th}$ , where  $i = x, y, z$ , is given by a Maxwell-Boltzmann velocity distribution as

$$f(v_i^{th}) = \sqrt{\frac{m}{2\pi T_0}} \exp\left[-\frac{(v_i^{th})^2}{2 \cdot (T_0/m)}\right], \quad (7)$$

where  $T_0$  is the input parameter in the model. The total velocity  $\vec{v}$  is the sum of these two velocity vectors,  $\vec{v} = \vec{v}^{th} + \vec{v}^{rd}$ . For a given parameter set of  $k$  and  $T_0$  values, which are determined below, the temperature is evaluated using the fluctuation thermometer and the extracted temperature values are shown in Fig. 3(a) for the thermal motion only,  $T_{th}$  (solid curve), and for the sum of the thermal motion and radial motion,  $T_{th+rd}$  (dashed curve). As expected, the temperature values for the thermal motion show a constant temperature. The temperature with the radial flow does not increase linearly as  $A$  increases because of the condition on the radial distance of the fragments  $r \leq r_{sys} - r_A$ . In order to apply this model to the reaction events, the momentum conservation,  $\sum_j m_j \vec{v}(j) = 0$ ; ( $j$  for all fragments in one event), has to be considered. In the actual application, among more than a hundred million events used in Fig. 3(a), only those with  $|\sum_j m_j \vec{v}(j)| \leq 100$  MeV/c are selected as an approximation of  $\sum_j m_j \vec{v}(j) = 0$ . When the momentum conservation of the system is required, the momenta of the larger fragments tends to be limited in smaller side relative to those of  $\vec{v} = \vec{v}^{th} + \vec{v}^{rd}$  used in Fig. 3(a). The results are shown by solid and dashed lines in Fig. 3(b). The parameters  $T_0$  and  $k$  are adjusted to reproduce the fluctuation temperature,  $T_{Q_{xy}}$  extracted from the AMD events in Fig. 3(b). As seen in the figure,  $T_{th}$  and  $T_{th+rd}$  show additional significant decreasing trends for heavier fragments, compared to those shown in Fig. 3(a). Using the parameter sets of  $T_0 = 4.9$  MeV and  $k = 0.024$  c/fm ( $k = 0.019$  c/fm without Coulomb), the  $T_{Q_{xy}}$  values from both AMD calculations with and without Coulomb are reproduced reasonably well by  $T_{th+rd}$  for  $A \geq 4$ . At the same time,  $T_{th}$ , the radial flow corrected temperature, reproduces well the temperature values of  $T_{sym}$  from the self-consistent symmetry energy analysis of the AMD events.

From the above Monte-Carlo simulation, the aver-

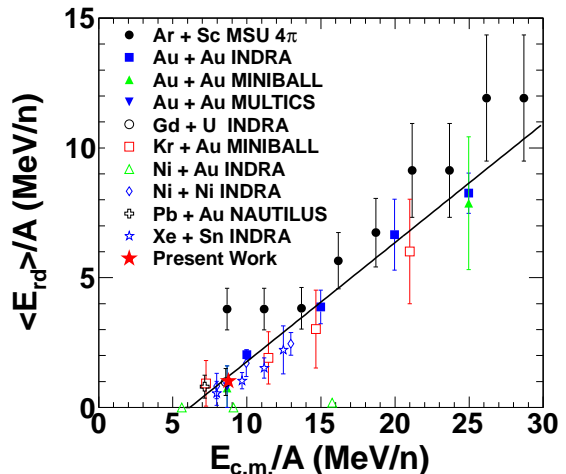


FIG. 4: (color online) Radial flow energy vs the incident energy. The experimental data are taken from Ref. [36].

age radial flow energy is evaluated as  $\langle E_{rd} \rangle = 1.02$  MeV/nucleon from Fig. 3(b). The average Coulomb repulsive energy is evaluated as  $\langle E_{Coul} \rangle = 0.61$  MeV/nucleon. Since the radial flow energy is not modified by the secondary decay cooling process, the extracted radial flow energy in the above analysis can be compared to the existing experimental data as shown in Fig. 4. Most of the existing data are distributed along the line  $\langle E_{rd} \rangle = 0.46(E_{c.m.} / A - 6.1)$  and, as seen in the figure, the extracted radial flow energy is consistent with that trend.

## V Conclusions and Summary

From the temperature values extracted above, the following conclusions are drawn:

- (1) The temperature values from the self-consistent symmetry energy analysis show a monotonic decrease of the temperature as the fragment mass  $A$  decreases from  $T \sim 5$  MeV at  $A = 8$  to  $T \sim 3$  MeV at  $A = 36$ .
- (2) The fluctuation thermometer gives higher temperature values, compared to those from the temperature extracted from the self-consistent symmetry energy analysis. They show a structure, i.e., a high temperature ( $T \sim 10$  MeV) for  $A = 1$ , which may originate from pre-equilibrium emission, a broad peak at  $A \sim 12$  and a monotonic decrease for larger  $A$ . Those from the AMD events without the Coulomb interaction show a similar trend but exhibit about  $1 \sim 1.5$  MeV lower values.
- (3) After the correction for the radial flow demanding momentum conservation in a Monte-Carlo

model, the behavior of the fluctuation temperature values are well understood as the combination of the thermal and radial motions. The bell shape structure of the temperature values of the raw fluctuation thermometer and the decreasing trend of those from the self-consistent symmetry energy analysis are well reproduced by the model. This indicates that the fluctuation thermometer can be a reasonable probe to measure the temperature of the fragmenting system in a multi-fragmentation process, if one can properly correct the contribution of the collective motion. We emphasize again that the fluctuation temperature employed is based upon the assumption of a classical momentum distribution.

Summarizing, an improved method for the extraction of the ratio of the symmetry energy coefficient relative to the temperature,  $a_{sym}/T$ , is applied for AMD events generated for  $^{40}\text{Ca} + ^{40}\text{Ca}$  at 35 MeV/nucleon. Gogny interactions, g0, goAS and g0ASS, with three different density dependencies of the symmetry energy are employed. As a function of IMF charge the ratios of the extracted  $a_{sym}/T$  values from the different interactions are essentially constant and reflect the differences of the symmetry energy at the density at the time of the fragment formation. Using this correlation,  $\rho/\rho_0 = 0.66 \pm 0.02$  is evaluated as the density at which the fragment formation occurs and the symmetry energy value at that density are extracted for each interaction. The temperature values are then determined. The extracted temperatures show a monotonic decrease as the fragment mass  $A$  increases, changing from 5 MeV to 3 MeV when  $A$  increases from 8 to 36. The extracted temperature values are compared to those of the fluctuation thermometer, which shows significantly higher temperature values and a different trend with fragment mass. After the correction for the radial flow the trends and the differences are well understood as resulting from the combination of the thermal and radial motions. This indicates that the fluctuation thermometer based upon the assumption of a classical momentum distribution provides a reasonable probe for the temperature of the multi-fragmentation source if the contribution of collective flows is properly corrected.

#### ACKNOWLEDGMENTS

X.Liu and W. Lin thank Prof. J. B. Natowitz for his hospitality during the stay in the Cyclotron Institute, TAMU. This work is supported by the National Natural Science Foundation of China (Grants No. 11075189) and

100 Persons Project (0910020BR0, Y010110BR0) and ADS project 302 (Y103010ADS) of the Chinese Academy of Sciences, the U.S. Department of Energy under Grant No. DE-FG03-93ER40773 and the Robert A. Welch Foundation under Grant A0330.

---

\* E-mail at:liuxingquan@impcas.ac.cn

† E-mail at:wada@comp.tamu.edu

- [1] Bao-An. Li *et al.*, Phys. Rep. **464**, 113 (2008).
- [2] M. B. Tsang *et al.*, Phys. Rev. Lett. **86**, 5023 (2001).
- [3] M. B. Tsang *et al.*, Phys. Rev. Lett. **92**, 062701 (2004).
- [4] M. A. Famiano *et al.*, Phys. Rev. Lett. **97**, 052701 (2006).
- [5] T. Li *et al.*, Phys. Rev. Lett. **99**, 162503 (2007).
- [6] A. Klimkiewicz *et al.*, Phys. Rev. **C76**, 051603 (2007).
- [7] L. Trippa *et al.*, Phys. Rev. **C77**, 061304 (2008).
- [8] Z. Kohley *et al.*, Phys. Rev. **C85**, 064605 (2012).
- [9] H. S. Xu *et al.*, Phys. Rev. Lett. **85**, 716 (2000).
- [10] M. B. Tsang *et al.*, Phys. Rev. **C64**, 054615 (2001).
- [11] M. Huang *et al.*, Nucl. Phys. **A847**, 233 (2010).
- [12] M. Huang *et al.*, Phys. Rev. **C81**, 044620 (2010).
- [13] M. Huang *et al.*, Phys. Rev. **C82**, 054602 (2010).
- [14] M. E. Fisher, Rep. Prog. Phys. **30**, 615 (1967).
- [15] R. W. Minich *et al.*, Phys. Lett. **B118**, 458 (1982).
- [16] A. S. Hirsch *et al.*, Nucl. Phys. **A418**, 267c (1984).
- [17] A. Bonasera *et al.*, Phys. Rev. Lett. **101**, 122702 (2008).
- [18] G. D. Westfall *et al.*, Phys. Lett. **B116** 118, (1982).
- [19] B. V. Jacak *et al.*, Phys. Rev. Lett. **51**, 1846 (1983).
- [20] S. Wuenschel *et al.*, Nucl Phys **A843**, 1, (2010).
- [21] S. Albergo *et al.* Nuovo Cimento **A89**, 1, (1985).
- [22] D. J. Morrissey *et al.*, Phys. Lett. **B148**, 423 (1984).
- [23] C. Guo and F. Zhang, Nuclear Science and Techniques **24**, 050513 (2013).
- [24] W. Lin *et al.*, Pjys. Rev. **C89**, 021601(R) (2014).
- [25] A. Ono *et al.*, Phys. Rev. **C59**, 853 (1999), *ibid* **C66**, 014603 (2002).
- [26] A. Ono, P. Danielewicz *et al.*, Phys. Rev. **C68**, 051601(R) (2003). For g0AS,  $x=-1/2$  and for g0ASS  $x=-2$  are used in Eq.(2) in Ref. [26].
- [27] A. Bonasera *et al.*, Riv. Nuovo Cimento **23**, 1 (2000).
- [28] C. F. von Weizsäcker, Z. Phys. **96**, 431 (1935).
- [29] H. A. Bethe, Rev. mod. Phys. **8**, 82 (1936).
- [30] M. Colonna, A. Ono and J. Rizzo, Phys. Rev. **C82**, 054613 (2010).
- [31] J. Rizzo, M. Colonna and A. Ono, Phys. Rev. **C76**, 024611 (2007).
- [32] W. Trautmann *et al.*, Phys. Rev. **C76**, 064606 (2007).
- [33] H. Zheng and A. Bonasera, Phys. Lett. **B696**, 178, (2011).
- [34] H. Zheng, G. Giuliani and A. Bonasera, Nucl. Phys. **A892**, 43, (2012).
- [35] D. Staufner, Phys. Rep. **54**, 1 (1979),  $p=0.28$  is used. The other choice of  $p$  does not change the results.
- [36] B. Borderie and M. F. Rivet, Prog. Part. Nucl. Phys. **61**, 551 (2008) and see references therein.